engineering proceedings

Proceeding Paper

Dual-Redundant Broadband Low-Noise Amplifier Module for Inter-Satellite Links at V-Band †

Peiman Parand [1], Hermann Barbato [1], Patrick Ettore Longhi [1,*], Alessandro Barigelli [2], Francesco Vitulli [2] and Ernesto Limiti [1]

[1] Electronic Engineering Department, University of Rome "Tor Vergata", Microwave Engineering Center for Space Applications, Via del Politecnico 1, 00131 Rome, Italy
[2] Thales Alenia Space Italia, Via Tiburtina, 00133 Rome, Italy
* Correspondence: longhi@ing.uniroma2.it
† Presented at the 15th EASN International Conference, Madrid, Spain, 14–17 October 2025.

Abstract

This paper presents the design and simulation of a dual-redundant broadband low-noise amplifier (LNA) module for inter-satellite communication links operating in the V-band (59–71 GHz). The growing demand for high-capacity space communication systems requires highly reliable, low-noise front-end architectures capable of maintaining performance over long mission lifetimes. To address these needs, a selectable dual-input receiver architecture is proposed, integrating a waveguide dual-probe, redundant switching, and a two-stage LNA within a single Gallium Arsenide (GaAs) MMIC. The design methodology accounts for the non-ideal behavior of the redundant branch and its impact on noise figure and insertion loss. The front-end is implemented using a 70 nm GaAs mHEMT technology optimized for millimeter-wave low-noise applications. Simulations show an insertion gain higher than 15 dB across the operational band, with gain ripple below 1.3 dB peak-to-peak. The simulated system noise figure is approximately 3.0 dB, closely matching the target specification. The results demonstrate that the proposed architecture provides improved reliability through redundancy while maintaining competitive noise and gain performance for future V-band inter-satellite links.

Keywords: V-band; SATCOM; low-noise receivers; Gallium Arsenide; MMIC; waveguide probe; WR-15

1. Introduction

The rapid growth of data-intensive space applications, including broadband satellite communications, Earth observation, and deep-space missions, has driven increasing interest in millimeter-wave frequency bands. In particular, the V-band (50–75 GHz) offers wide available bandwidths that enable high-capacity links, reduced spectral congestion, and improved frequency reuse compared to traditional microwave bands. However, operation at these frequencies introduces significant technical challenges related to component integration, and system reliability, which require advanced solutions in both microwave hardware and antenna technologies [1].

Millimeter-wave microwave components operating in the V-band are critical enablers of next-generation space telecommunication systems [2]. Key building blocks include low-loss waveguides and ultra-low-noise front-end receiver chains. Among these, low-noise receive systems play a decisive role in determining overall link performance. The

Check for updates

Academic Editors: Spiros Pantelakis, Andreas Strohmayer and Gustavo Alonso

Published: 9 May 2026

Copyright: © 2026 by the authors. Licensee MDPI, Basel, Switzerland. This article is an open access article distributed under the terms and conditions of the Creative Commons Attribution (CC BY) license.

design of low-noise amplifier (LNA) must balance stringent noise figure requirements with constraints on power consumption. Advanced semiconductor technologies such as III–V compound semiconductors and emerging SiGe platforms, have become essential to achieve the necessary noise and gain performance at V-band frequencies [3].

Beyond raw performance, system reliability has become a central design driver for spaceborne V-band communication payloads [4,5]. Redundancy is particularly important in this context, as on-orbit maintenance is not feasible and mission lifetimes may extend over many years. One of the most effective architectural strategies to enhance reliability is the incorporation of selectable dual-input receiver microwave systems. Such architectures typically employ redundant RF front-ends, including parallel LNAs, switches, and signal routing networks, allowing seamless reconfiguration in the event of component degradation or failure. By introducing hot- or cold-standby receiver paths and highly reliable RF switching mechanisms, these systems can significantly increase operational availability while maintaining stringent noise and linearity requirements.

In this paper, we present the analysis and design of a dual-input waveguide probe integrated onto a single MMIC comprising redundancy switch and the LNA.

A receiver architecture is proposed with an emphasis on low-noise microwave component design, waveguide-to-microstrip probe integration, and robust redundancy strategies based on selectable dual-input receiver systems. The work aims to demonstrate how carefully engineered redundancy at the microwave front-end level can substantially improve system resilience without unacceptable penalties in mass, power consumption, or noise performance, thereby enabling more reliable high-capacity space communication links in future satellite and deep-space missions.

The presented research activity is performed within the framework of ESA's dual-redundant broadband low-noise amplifier module for inter-satellite links at V-band (DUreL-V) project as a follow-on of an earlier ESA study performed at a lower frequency, and more in particular at Q-band [6].

2. Dual-Redundant Receiver Architecture

The baseline architecture of the dual-redundant LNA is presented in Figure 1. All the functional blocks have been partitioned into realizable MMICs, the discontinuities are identified, and the parts in the waveguide specified as well. The line-up is well-consolidated by Thales Alenia Space in Italy and largely flight-proven. The input is in WR15 waveguide and hosts the dual-probe arrangement to allow the splitting of the RF input. Two front-end MMICs follow, one per RF chain. The front-end MMIC carries on the probe (patch antenna) protruding into the waveguide, a SPST (Single-Pole Single-Throw) switch in redundant configuration (two in parallel) and a two-stage LNA. The NF of this fundamental first active item is determined by the following contributions:

1. Losses of the probe and $\lambda/4$ line realized onto the GaAs substrate, including the effect of the non-perfect short circuit of the switch in the OFF branch of the module;
2. Losses due to the SPST in ON state;
3. NF of the single-stage LNA, exhibiting an associated gain of approximately 18 dB.

A three-stage LNA MMIC follows to improve the gain of the system. A passive flatness equalizer is inserted to correct the in-band amplitude response, if needed. Such an equalizer also provides a mild filtering action to aid the output filter and reduce the noise bandwidth after the first amplifier. To compensate for temperature-induced gain variation, a Voltage Variable Attenuator (VVA) is included in the RF chain, driven by a thermistor-based resistive network implemented on an ancillary PCB. A balanced MMIC amplifier follows, having the task of linearly amplifying the signal (with 20 dB gain), and providing a matched termination to the following combiner. The recombination of the two

https://doi.org/10.3390/engproc2026133112

RF chains outputs is performed via a waveguide branch-line combiner, featured by low losses and robust performance. To launch the RF signal into the waveguide, a transition is necessary, implemented with a probe on the ceramic substrate.

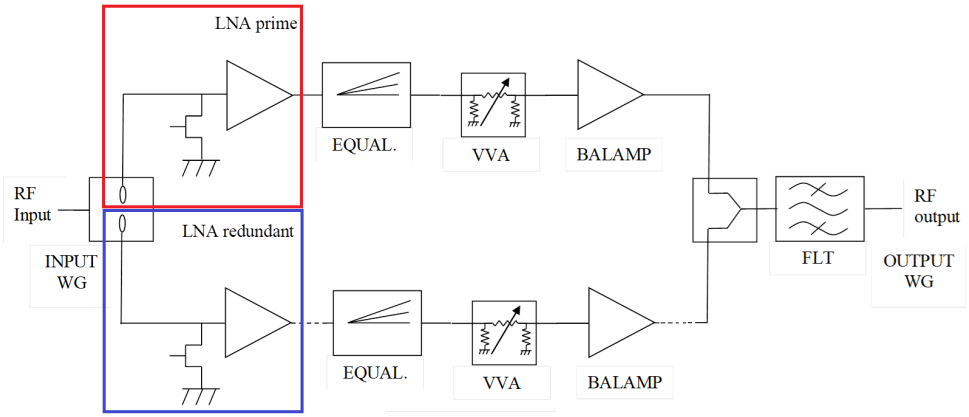

Figure 1. Architectures for dual-redundant LNA unit in V-band. The MMIC described in this paper appears in the red and blue boxes. The MMICs have identical electrical schematics and are alternatively switched on and off for redundancy.

3. Front-End Sub-Circuit Design

The V-Band front-end MMIC is depicted in the coloured boxes in Figure 1. The MMIC design is accomplished by taking into account the effects of the dual probe inside the input waveguide. This component must be carefully analyzed and designed so its lossy and noisy effects are correctly accounted for. Ideally the "switched-off" branch will show an ideal open circuit to the probe, consequently isolating the branch and not injecting any noise into the operating branch. However, the OFF-state SPST cannot, at the V-band, provide an ideal short and consequently some input power will leak into the "switched-OFF" channel. This power leak corresponds to higher losses and noise in the "switched-ON" channel. In the following sections, we will present design guidelines and the simulated performance of the three VB FE sub-circuits:

1. Dual-input probe;
2. SPST switch;
3. Two-stage LNA.

The following subsections contain design information of the three subcircuits enumerated in the previous list together with an indication of the selected technology. Finally, the design bandwidth is 59–71 GHz.

3.1. Selected Gallium Arsenide MMIC Technology

Several advanced III–V technologies are available for low-noise applications at millimetre-wave frequencies [7]. Gallium nitride multi-function MMICS (LNA and switch) have been demonstrated at the Ka-band [8]. However, the MMIC technology selected for this design is MACOM's (formerly OMMIC) 70 nm Gallium Arsenide (GaAs) HEMT. D007IH is a 70 nm mHEMT technology process that is fully available for production in three-inch wafers. The process is optimized for ultra-low-noise applications up to 150 GHz. Its main RF and DC characteristics are V_{bgd} 4 V (typical), f_T of 300 GHz, and f_{MAX} of 450 GHz. A full set of passives is available as: epitaxied resistors, NiCr resistors MIM capacitors, spirals, air bridges, via holes, and microbumps. Substrate thickness is 0.1 mm with 0.07 mm optional. This process is space-evaluated and EPPL-listed by ESA.

https://doi.org/10.3390/engproc2026133112

3.2. Dual-Input Probe

The probe element is designed using the radial stub topology [9]. The ground plane is removed beneath the radial stub. An appropriately sized transmission line is inserted to re-phase the load provided by the switched-OFF channel. The SPST is connected at the output of this section. A dedicated simulation environment is prepared to evaluate the effect of both the ON and OFF switches on the overall receiver performance, as shown in Figure 2. It should be noted that the ON-state switch degrades the receiver noise figure through its finite ohmic (insertion) loss, while the OFF-state switch contributes to the overall noise figure by coupling noise from the inactive branch into the active signal path, due to the non-ideal open-circuit behavior of the switch at the V-band. Further details on the switch design are reported in Section 3.3.

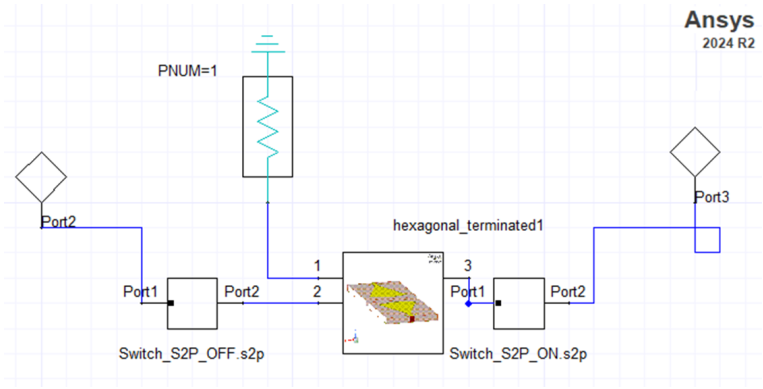

Figure 2. Equivalent circuit schematic used to analyze and design the dual-input probe's radiating element.

Quite obviously, the ideally terminated probe shows better performance than the "real-case" counterpart. The RF behaviour in the real-case is approximately 0.6 dB worse than the ideal case. The insertion loss of the ideally-terminated probe is 0.2 dB against the 0.8 dB of the SPST-terminated probe.

3.3. Switch Design

The switch is designed using a dual-redundancy configuration. Therefore, two FETs are required to provide redundancy functionality. A simplified schematic of the redundancy switch is given in Figure 3.

The solution in Figure 3 uses a quarter wavelength section of transmission line as impedance transformer [10]. When both transistors are in the on state, they lower the impedance at the end of the $\lambda/4$ line (close to port 2) which is transformed to high impedance at the input, port 1. That isolates this branch of the switch. In the opposite operating mode, the transistors are in off-state, and they are matched to line's characteristic impedance with parallel stubs (L_{stub}) implemented by short and thin transmission lines. The shunt stub lines are used to improve isolation of the off-state branch. This topology is widely used in most of the available RF switches, when the bandwidth is small to medium. A capacitor is added both for RF matching purposes and most of all to provide dc de-coupling between the FET switches and the LNA in case of LNA failure. To implement switch redundancy, two transistors are inserted instead of a single one. The gate terminal resistors are in the order of 3–5 kOhm to implement high RF isolation. The switch simulated insertion loss is in the order of 0.6 dB and directly impacts the receiver's NF.

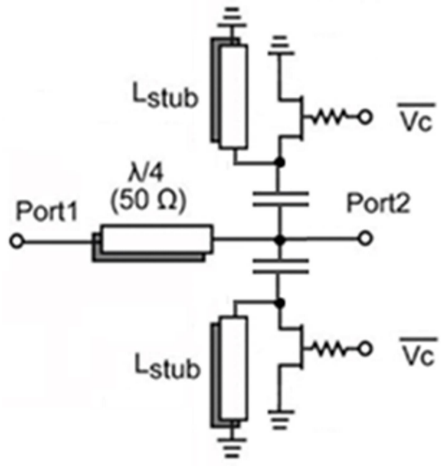

Figure 3. Schematic diagram of an SPST switch with shunt topology and FET redundancy (two shunt FETs instead of a single FET).

3.4. Low-Noise Amplifier Design

A two-stage LNA is designed and inserted into the V-band front-end MMIC. As stated previously, a two-stage topology is necessary to simultaneously fulfil the noise and signal match conditions at both LNA I/O ports. This condition cannot be fulfilled using a single stage approach and a poor level of output return loss would have to be accepted in the hypothesis of optimum noise and signal match at the single-stage LNA input port. The two-stage LNA is designed to target the following specifications: 59 to 71 GHz, 16 to 18 dB gain, and 1.6 dB NF. A two-stage topology is adopted as shown in the simplified electrical circuit in Figure 4. Additional design detail for the LNA section are given in [11–14].

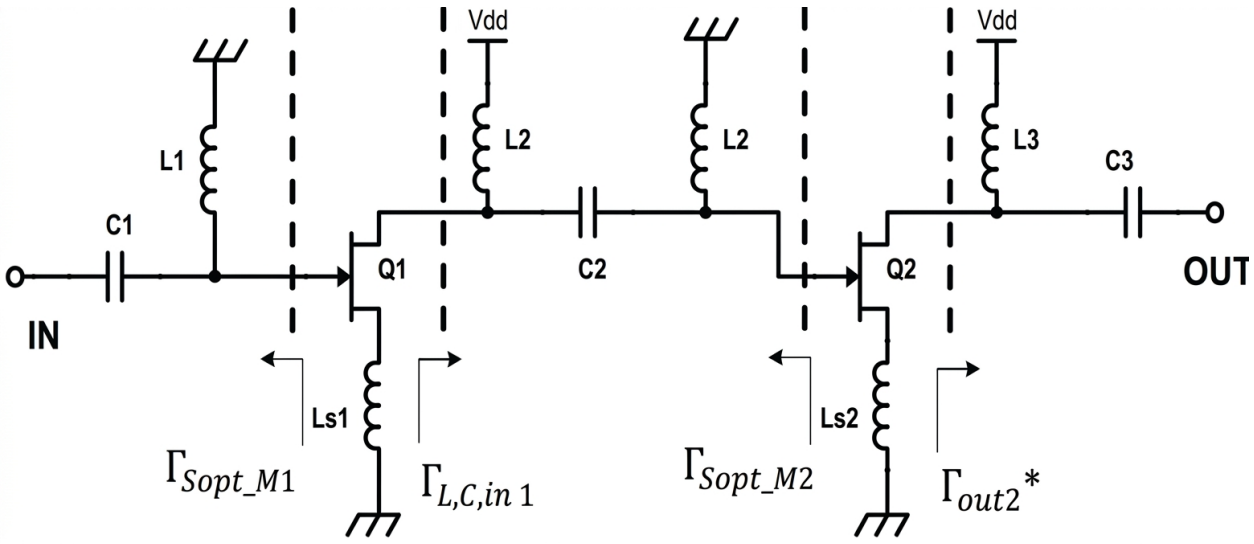

Figure 4. Simplified schematic diagram of the two-stage LNA.

4. Front-End MMIC Design and Simulation

4.1. Front-End MMIC Design

The front-end MMIC is designed assembling the sub-circuits described in the previous sections and integrating them into a single design environment. Obviously, the effect of the OFF-state branch must be account for in design and simulation. For this reason, a specific design schematic is developed and provided in Figure 5. The same picture in inset (b) reports the MMIC implementation on the V-band front-end.

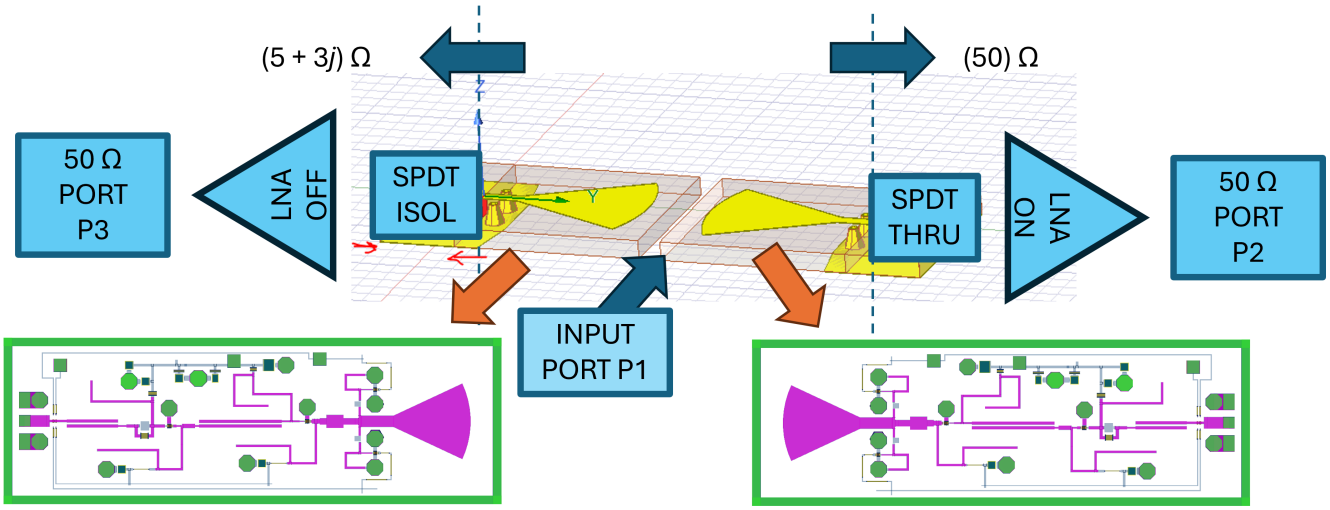

Figure 5. Simplified block diagram used to generate the simulations reported in this section. The V-band front-end MMIC layout is reported and the arrows indicate the correspondence between simulation element and physical layout.

4.2. Front-End MMIC Simulation

Figure 6 reports the linear and noise parameters from the waveguide input port to the output port of the MMIC VB FE. As stated previously, this gain accounts for the losses introduced by the disabled branch of the receiver. Insertion gain (bottom-left plot) is higher than 15 dB. The ripple is rather flat, less than 1.3 dB pk-to-pk.

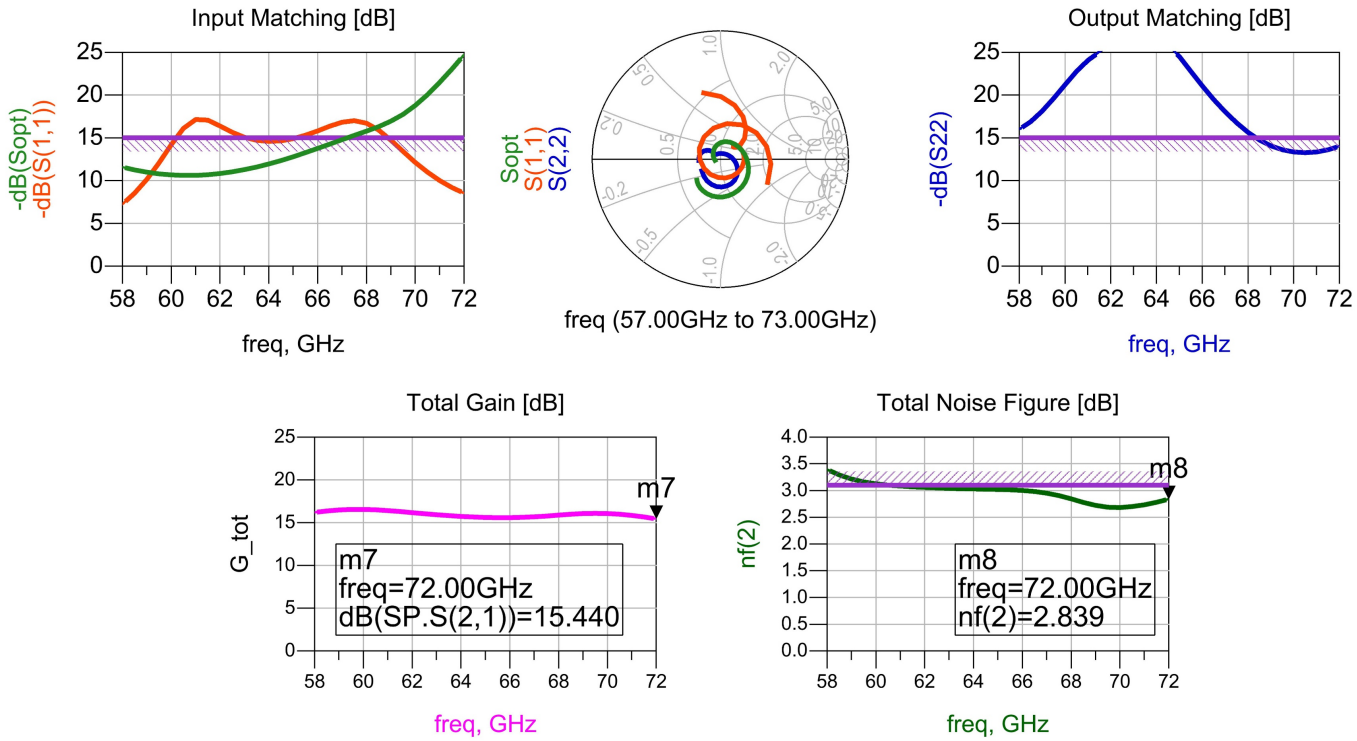

Figure 6. Top row: Simulated input and output return loss, and the corresponding Smith chart representation. Bottom row: Simulated Insertion gain (left) and noise figure (right) of the receiver subsystem (from waveguide input to VB FE MMIC output).

Figure 6 reports the noise figure (bottom right plot) when port 1 is the waveguide input port and port 2 is the output port of the two-stage LNA. As stated previously, this

noise figure accounts for the losses and noise introduced by the disabled branch of the receiver. The simulated NF of the receiver system is typically 3.0 dB against the 2.8 dB specification. This is due to the higher NF of the input probe. The target specification is 0.6 dB but, at the moment, we are simulating 0.7–0.9 dB. The other two sub-circuits (SPST and LNA) have noise figures in-line with budget requirements. Finally, the top-row plots in Figure 6 report the matching, which is better than 10 dB over the operating bandwidth.

5. Discussion

The presented results demonstrate that the proposed dual-redundant front-end architecture is a viable solution for highly reliable V-band receiver systems. Compared with conventional single-path LNA front-ends, the inclusion of a redundant input branch inevitably introduces additional losses and noise contributions due to non-ideal switch isolation and probe behavior. However, the simulations show that these penalties remain limited and compatible with stringent system requirements for inter-satellite links. The achieved gain flatness and overall insertion gain confirm the effectiveness of the integrated equalization and matching strategies.

The slightly degraded noise figure, primarily driven by the input probe and the finite isolation of the OFF-state branch, highlights the importance of accurate co-design between waveguide transitions and MMIC circuitry at millimeter-wave frequencies. The results are consistent with previously reported work in Q-band redundant receivers, while extending the concept toward fully integrated, compact MMIC implementations. Future work should focus on experimental validation, thermal and radiation characterization, and further optimization of the probe and switch structures to approach the targeted noise figure. These improvements will be critical for next-generation high-capacity and long-lifetime space communication payloads.

6. Conclusions

A dual-redundant broadband LNA module for V-band inter-satellite communication links has been designed and analyzed. The proposed architecture integrates a dual-probe waveguide interface, redundant SPST switching, and a two-stage low-noise amplifier in a single GaAs MMIC, enabling improved system reliability without excessive penalties in terms of mass, power consumption, or RF performance. The simulation results demonstrate an insertion gain exceeding 15 dB across the 59–71 GHz band and a relatively flat gain response, confirming the effectiveness of the adopted matching and equalization techniques. The simulated noise figure of approximately 3.0 dB is close to the target specification and is mainly limited by the input probe and switch non-idealities.

The study confirms that redundancy can be successfully implemented at the microwave front-end level while preserving competitive electrical performance. The proposed solution represents a promising building block for future high-capacity, resilient inter-satellite links operating at millimeter-wave frequencies. Further work will include fabrication and experimental validation, as well as environmental testing for space qualification.

Author Contributions: Conceptualization, P.P., H.B. and P.E.L.; methodology, all; investigation, A.B.; writing—original draft preparation, P.E.L.; writing—review and editing, all; project administration, F.V.; funding acquisition, E.L. All authors have read and agreed to the published version of the manuscript.

Funding: This research was funded by European Space Agency grant number AO/1-11622/23/NL/EG "Dual-redundant broadband low noise amplifier module for inter-satellite links at V-band" whose

support is gratefully acknowledged. The views expressed in this publication can in no way be taken to reflect the official opinion of the European Space Agency.

Data Availability Statement: Data is available on request.

Conflicts of Interest: The authors Francesco Vitulli and Alessandro Barigelli are employed by the company Thales Alenia Space in Italy. The remaining authors declare that the research was conducted in the absence of any commercial or financial relationships that could be construed as potential conflicts of interest.

References

1. Aloisio, M.; Angeletti, P.; Coromina, F.; De Gaudenzi, R. Technological challenges of future broadband telecommunication satellites in Q/V-band. In *2012 IEEE International Conference on Wireless Information Technology and Systems (ICWITS)*; IEEE: New York, NY, USA, 2012; pp. 1–4. [CrossRef]
2. Kodheli, O.; Lagunas, E.; Maturo, N.; Sharma, S.G.; Rao, B.; Montoya, J.F.M.; Merlano-Duncan, J.; Spano, D.; Chatzinotas, S.; Kisseleff, S.; et al. Satellite Communications in the New Space Era: A Survey and Future Challenges. *IEEE Commun. Surv. Tutor.* **2021**, *23*, 70–109. [CrossRef]
3. Tessmann, A.; Leuther, A.; Thome, F.; John, L.; Gashi, B.; Massler, H.; Saam, A.; Chartier, S. Advanced mHEMT Technologies for Use in Radar, Communication and Meteorological Applications. In *2023 IEEE BiCMOS and Compound Semiconductor Integrated Circuits and Technology Symposium (BCICTS)*; IEEE: New York, NY, USA, 2023; pp. 219–224. [CrossRef]
4. Park, S.R.; Nguyen, R.N.; Nguyen, S.T.; Chiang, N.H.; Sowers, J.J. V-band receiver for commercial space applications. In *2017 IEEE MTT-S International Microwave Symposium (IMS)*; IEEE: New York, NY, USA, 2017; pp. 1830–1833. [CrossRef]
5. Ladkani, J.; Agarwal, N.; Thakkar, J.; Jain, A.; Singh, D.K. Space Qualified Q/V Band Receiver for High Throughput Communication Satellites. In *2022 IEEE Microwaves, Antennas, and Propagation Conference (MAPCON)*; IEEE: New York, NY, USA, 2022; pp. 259–263. [CrossRef]
6. Kotiranta, M.; Henneberger, R.; Bruch, D.; Lia, E.; Leuther, A.; Massler, H.; Schlechtweg, M. Dual waveguide probe based redundant Q/V-band low-noise amplifier. In Proceedings of the ESA Microwave Week, Noordwijk, The Netherlands, 3–5 April 2017; pp. 1–8.
7. Samoska, L.A.; Varonen, M.; Kangaslahti, P.; Fung, A.; Gawande, R.; Soria, M.; Lai, R.; Sarkozy, S. V-band MMIC LNAs and mixers for observing the early universe. In *2016 41st International Conference on Infrared, Millimeter, and Terahertz Waves (IRMMW-THz)*; IEEE: New York, NY, USA, 2016; pp. 1–2. [CrossRef]
8. Haque, S.; Andrei, C.; Wolf, M.; Hilt, O.; Rudolph, M. Switch Integrated Ka-Band Low Noise Amplifier in GaN/AlN HEMT Technology. In *2024 19th European Microwave Integrated Circuits Conference (EuMIC)*; IEEE: New York, NY, USA, 2024; pp. 351–354. [CrossRef]
9. Han, M.; Wang, C.; Liu, C.; Xiao, S.; Ma, J.; Sun, H. A Wideband Microstrip-to-Waveguide Transition Using E-Plane Probe with Parasitic Patch for W-Band Application. *Appl. Sci.* **2022**, *12*, 12162. [CrossRef]
10. Thome, F.; Leuther, A.; Ambacher, O. Low-Loss Millimeter-Wave SPDT Switch MMICs in a Metamorphic HEMT Technology. *IEEE Microw. Wirel. Compon. Lett.* **2020**, *30*, 197–200. [CrossRef]
11. Salvucci, A.; Longhi, P.E.; Colangeli, S.; Ciccognani, W.; Serino, A.; Limiti, E. A straightforward design technique for narrowband multi-stage low-noise amplifiers with I/O conjugate match. *Int. J. Microw. Comput.-Aided Eng.* **2019**, *29*, e21833. [CrossRef]
12. Longhi, P.E.; Pace, L.; Colangeli, S.; Ciccognani, W.; Leblanc, R.; Limiti, E. V-Band GaAs Metamorphic Low-Noise Amplifier Design Technique for Sharp Gain Roll-Off at Lower Frequencies. *IEEE Microw. Wirel. Compon. Lett.* **2020**, *30*, 601–604. [CrossRef]
13. Ciccognani, W.; Longhi, P.E.; Colangeli, S.; Limiti, E.; Senior Member IEEE. Q/V band LNA for satellite on-board space applications using a 70 nanometers GaAs mHEMT commercial technology. *Microw. Opt. Technol. Lett.* **2018**, *60*, 2185–2190. [CrossRef]
14. Ciccognani, W.; Colangeli, S.; Longhi, P.E.; Limiti, E. Design of a MMIC low-noise amplifier in industrial gallium arsenide technology for E-band 5G transceivers. *Microw. Opt. Technol. Lett.* **2019**, *61*, 205–210. [CrossRef]

Disclaimer/Publisher's Note: The statements, opinions and data contained in all publications are solely those of the individual author(s) and contributor(s) and not of MDPI and/or the editor(s). MDPI and/or the editor(s) disclaim responsibility for any injury to people or property resulting from any ideas, methods, instructions or products referred to in the content.